

A Comparison of Geospatial Interpolation Techniques for Gold Anomalies in Wassa-Amenfi District, Southwest of Ghana.

Abstracts

In spatial interpolation, the Inverse-Distance Weight (IDW) and Kriging methods are two of the most widely used deterministic and geostatistical models. In deterministic techniques, interpolation is performed using mathematical functions, whereas geostatistics uses both statistical and mathematical methods to create surfaces and assess the uncertainty of predictions. The goal of this paper is to compare the Kriging and IDW spatial interpolation methods in the Wassa-Amenfi District using gold concentration data collected by the Ghana Geological and Survey Authority. The prediction accuracy of the spatial interpolation models was improved by reducing the complexity of the time series gold concentration dataset using the logarithm and Box-Cox data transformation method. The performance of these methods is measured using the Root Mean Square Error (RMSE). Kriging model R^2 of 0.92 and 0.81 in both Box-Cox and logarithm transformed Au datasets were greater than IDW R^2 squares of 0.78 and 0.87. As a result, the kriging method outperformed the IDW and was found to be the best interpolation technique for mapping and predicting gold concentration anomalies in the Wassa-Amenfi District, located in Southwest Ghana.

Keywords: Inverse Distance Weight, Kriging, gold, Interpolation

1.0 Background

Mining projects relating to precious metals such as Gold (Au) deposits, require accurate information on tonnage and grade to ensure credible resource estimates and good project feasibility [1,2,3]. This requirement has become very crucial in recent years, due to the negative impacts of increasing depletion of high-profit deposits, unstable world market prices, cost of production and weak legislation, among

other factors [4]. Notably, many companies failed to live up to expectations due to poor grade and tonnage estimations, as well as ineffective geological controls [5,6,7,8]. Accurate mineral resource and mineral reserve evaluations, therefore, form the basis on which economic decisions are made on mining project estimation have been mainly by polygonal method and a factor applied for error correction [9]. Though historically, these methods might have worked satisfactorily, there are also many drawbacks due to inherent assumptions that lead to overestimation [10].

Kriging and the Inverse Distance method are commonly used in spatial interpolation and prediction in geostatistical data modelling. Geostatistical modelling has its roots in the mining industry, where the model was used to estimate and interpolate metal grades in the study area. Because spatial processes are highly dependent, geostatistical models forecast using data from the nearest neighbours. In addition, the uncertainty measure associated with the prediction of the process at an unobserved location depends on the proximity of observed values of the process. The Inverse Distance Weight (IDW) has long been the most popular data interpolation technique. The IDW estimate is because any pair of points is dependent on each other, and their similarity is inversely proportional to the distance between them. According to [11], not all points' spatial dependencies are proportional to distance. In addition, IDW cannot estimate the variances of predicted values in unsampled locations as compared to what geostatistical methods such as kriging can provide [12]. Amadu et al. in 2014 used geostatistics to estimate a shear-hosted gold deposit at Obuasi, and their findings demonstrated the utility of geostatistics in determining the architecture of Au mineralization at the deposit scale. [13]

[14], use the Kriging and IDW methods to model gold anomalies in the North-Western part of Ghana. Their findings indicated that both methods used in the analysis showed no contradiction, indicating the same Au anomalies zones. However, before applying any spatial interpolation technique to any dataset, data normalization is required. According to a review of the literature, the most commonly used method of data transformation is the logarithm approach without any simulation to determine the best method of transformation. The Kriging and IDW methods were compared after a Box-Cox and logarithm transformation of gold concentration to determine the best spatial interpolation model and data transformation method. The robust model with the best data normality transformation method was used to interpolate gold concentration anomalies in the study area.

2.0 METHODS

2.1 Sample Data

For the study, two thousand, seven hundred and fifty (2,750) soil samples were collected on a grid basis at Adiembrain Wassa-Amenfi District using the soil auger drilling method at an average depth of 3 m. The gold concentration in parts per billion in these samples was determined by the Ghana Geological Survey Authority using graphite furnace atomic absorption spectrometry (GF-AAS) [15,16].

2.2 Study Area

Primary gold mineralization in Ghana occurs along shear zones composed of quartz veins within 240 km-long Birimian greenstone belts. There are at least four of these belts (Kibi-Winneba, Ashanti, Asankrangwa, and Sefwi) [17]. Gold quartz veins run across full-size primary orebodies, intensely entering fissures and shear zones at metasedimentary and metalvolcanic rock contacts. Quartz with carbonate minerals, inexperienced sericite, carbonaceous partings, and steel sulfides and arsenides of Fe, As, Zn, Au, Cu, Sb, and Pb predominate in the veins. According to [18], impervious isotope analyses of host-rock and ore factors showcase that mineral deposition took location all through elaborate multi-stage mineralization events, with higher temperature minerals deposited from dilute aqueous preferences to produce gold mineralization, which can be altered through a secondary dispersion mechanism. The Ashanti-Belt and which runs through the Wassa-Amenfi District is made up of three major geological soil formations: Upper Birimian, Lower Birimian, and Granites. The district's granite deposits are rich in minerals such as gold and iron, this is why the study area was chosen. The research region is depicted in Figure 1.

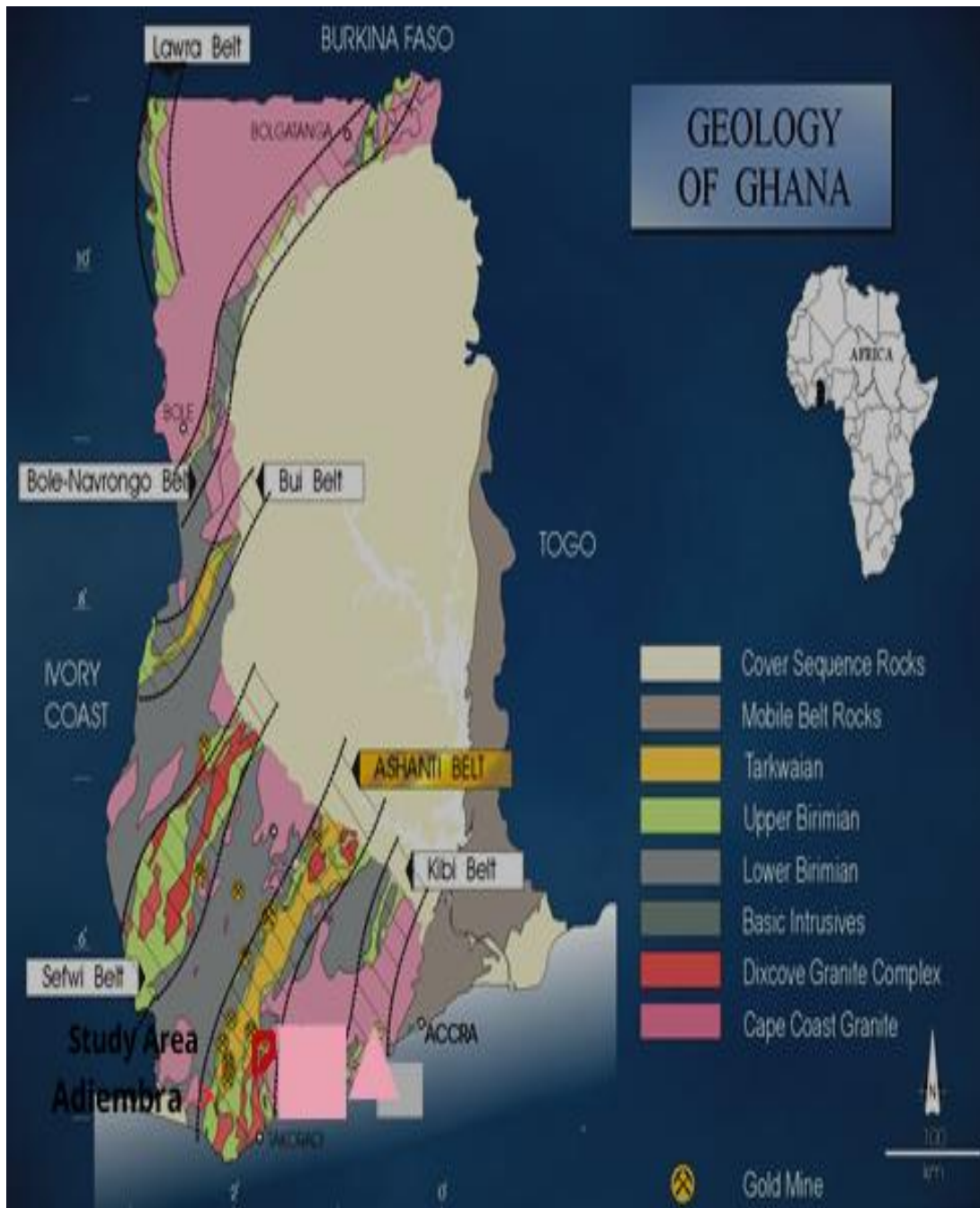


Figure 1: Concession map of the study area

2.3 Model Formulation

2.3.1 Semi Variogram

A variogram is a useful tool for describing the behaviour of non-stationary, spatially random processes. It is an "essential step" in geostatistics for analyzing spatial variability [19]. Kriging predicts the value of a function at a given point by computing a weighted average of the function's known values in the point's neighbourhood. The method is very similar to regression analysis. Calculations in several directions, such as, along strike, across strike and down dip directions give an insight into the structural and geometric controls on the orebody [20]. The variogram represents the variance between sample pairs as a function of the distance (lag) between the samples in a particular direction [21]. An experimental variogram, $\gamma(h)^*$ can be defined as [22]:

$$\gamma^*(h) = \frac{1}{2n} \sum_{i=1}^n \{Z(x_i) - Z(x_i + h)\}^2 \quad (1)$$

Where $Z(x_i)$ is the value of Au concentration at x_i , $Z(x_i + h)$ is the grade of the sample at distant h from the point x_i and n is the number of sample pairs.

2.3.2 Kriging Methods

Consider a collection of random variables $\{Z(s): s \in \mathcal{D} \subset \mathbb{R}^d\}$, which we refer to as a random spatial process. The mean function of the process $Z(\cdot)$ is defined as being $E[Z(s)] \equiv \mu_Z(s) s \in \mathcal{D}$, and the covariance function is defined as

$$C_Z(s_i, s_j) \equiv \text{cov}(Z(s_i), Z(s_j)) \quad (2)$$

for any $s_i \in \mathcal{D}$ and $s_j \in \mathcal{D}$. Both functions exist if we suppose that $\text{var}(Z(s)) < \infty$, exists for every $s \in \mathcal{D}$.

Spatial processes of the type described above serve as the foundation for statistical studies of geostatistical data. The kriging method is given by:

$Z_{new} = w_1 Z_1 + w_2 Z_2 + \dots + w_i Z_j + \mathcal{E}_{new}$, where w 's are weights that are applied to the Au concentration. Estimation of w 's:

$$w = \begin{pmatrix} \text{cov}(z_1, z_1) & \text{cov}(z_1, z_2) & \dots & \text{cov}(z_1, z_i) \\ \text{cov}(z_2, z_1) & \text{cov}(z_2, z_2) & \dots & \text{cov}(z_2, z_i) \\ \text{cov}(z_3, z_1) & \text{cov}(z_3, z_2) & \dots & \text{cov}(z_3, z_i) \end{pmatrix}^{-1} \begin{pmatrix} \text{cov}(z_{new}, z_1) \\ \text{cov}(z_{new}, z_2) \\ \text{cov}(z_{new}, z_3) \end{pmatrix} \quad (3)$$

2.3.3 Inverse Distance Weight

Inverse Distance Weight (IDW) interpolation uses a linearly weighted combination of a set of sample points to determine cell values. The weight is determined by the inverse distance. The interpolated surface should be that of a locationally dependent variable. Estimation of IDW is given equation (5)

$$Z_{new} = \frac{\lambda_1 Z_1 + \lambda_2 Z_2 + \dots + \lambda_i Z_i}{\lambda_1 + \lambda_2 + \dots + \lambda_i}, \quad (4) \text{ where } i, j=1, 2, \dots \text{ and } \lambda_i = \frac{1}{d_i^p} \quad (5)$$

where d denotes the distance between the unknown point and its nearest neighbours. The exponential power p is used to increase the weight of the nearest data point while decreasing the weight of the far data point.

2.4 Model Validation

The model was validated using cross-validation, which removes each sample value from the datasets and uses point kriging and IDW to re-estimate the sample value from the remaining data using the test model[23].

3.0 RESULTS AND DISCUSSIONS

3.1 Descriptive Analysis of Sample Data

Table 1 highlights the descriptive analysis of the data collected.

Table 1: Descriptive Analysis of Raw Gold Sampled

Mean	Maximum	Minimum	Std.	Skewness	Kurtosis
5.24	990.0	1.0	25.11	27.12	46.45

In general, the index's maximum and lowest Au contents are considerably distinct. A high standard deviation indicates that Au content varies greatly. Positive skewness is also apparent, showing that the right tail is especially severe, indicating non-symmetric yields for the Au concentration.

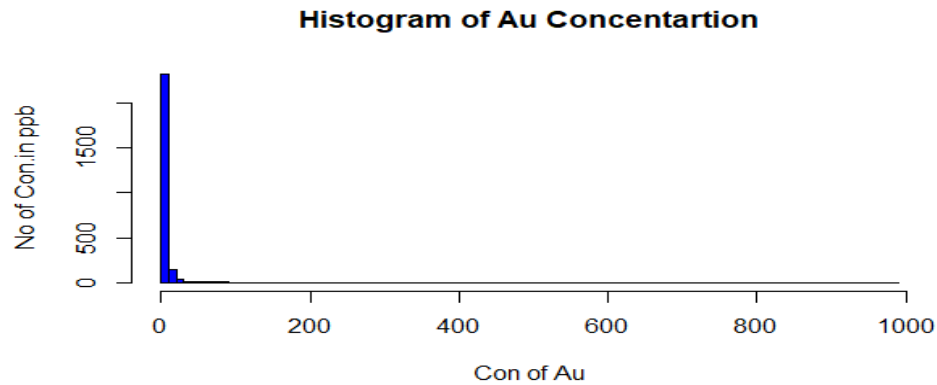


Figure 3: Histogram of Au concentration

The histogram in Figure 3 shows that the data is not symmetrically distributed. The dataset's right skewness and high kurtosis indicate that the distribution concentration of Au in the study field is not uniform, with the majority of the data values being the same and only a few data values having extreme Au concentration. Due to the spatial dependence of datapoints, geochemical datasets are not normally distributed [24].

3.2 Logarithm transformation

The logarithmic transformation reduced the mean and standard deviation data from 5.24 to 2.21 and 25.11 to 3.78, respectively. The skewness and kurtosis are now 1.96 and 3.95, respectively. The datasets were considered normally distributed because their skewness and kurtosis were within the acceptable ranges of skewness between -3 and +3 and kurtosis between -10 and +10 according to [25].

Table 2: Log transformation of Au Sampled

Mean	Maximum	Minimum	Std.	Skewness	Kurtosis
2.21	38.32	1.03	3.78	1.96	3.95

3.3 Box-Cox transformation

Thus, Box-Cox (BC) transformation was also applied to the dataset to obtain optimal parameters that will aid in data transformation. (Figure 3).

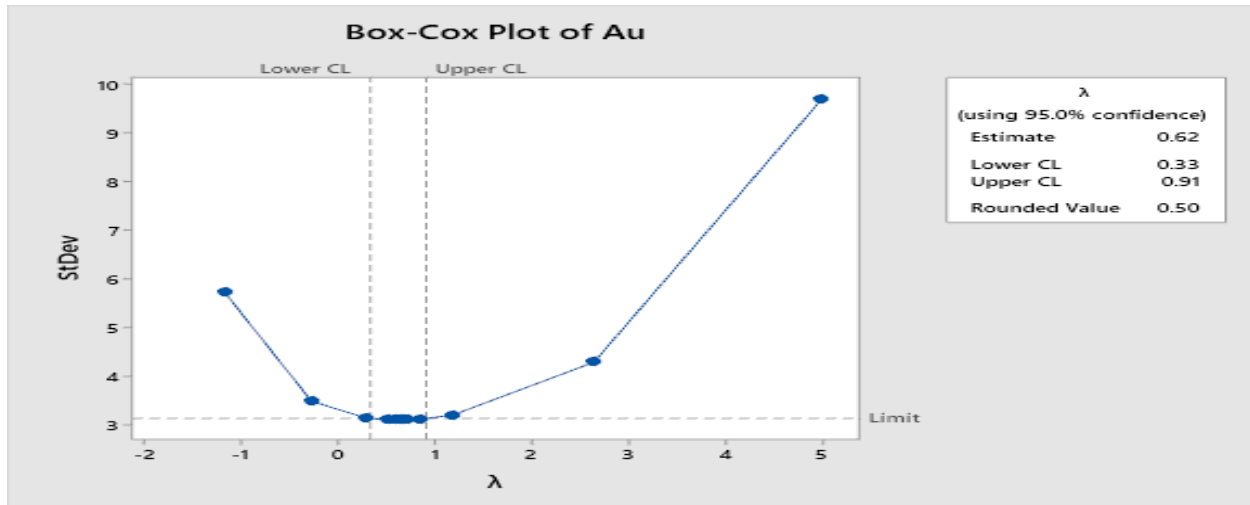


Figure 4: Box-Cox Plot of Au

In Figure 3, the estimated value for the optimal (λ) was 0.62. The obtained confidence intervals do not include 0, indicating that logarithm transformation would not be appropriate for the datasets. Furthermore, the rounded value of 0.5 falls within the confidence interval, implying that the best normality transformation would be achieved by square rooting the Au datasets. Table 3 summarizes the statistics of the Au dataset after being transformed with the square root.

Table 3: Summary Statistics using BC transformation of Au

Mean	Maximum	Minimum	Std.	Skewness	Kurtosis
1.72	31.46	1.00	1.52	1.42	2.45

The means in Table 3 after the BC transformation is now 1.72 instead of 5.24 before the transformation. Before the transformation, the standard deviation was 25.11; now, it is 1.516. According to [25], the skewness of 1.42 obtained in Table 4 falls within the range of data normality, although [26] stated that no dataset is perfectly normally distributed; rather, the data must be close to normal.

3.4 Model Performance Test

To determine the best model, the kriging and IDW models were compared using the two methods of data transformation.

Table 4: Model Comparison

	BC Kriging	Log kriging	BC IDW	Log IDW
RME	2.431	5.895	6.65	7.50
R²	0.93	0.82	0.79	0.74

The results show that Box-Cox (BC) kriging significantly improved Au concentration estimates by reducing the overall estimation error by 34% and increasing the coefficient of determination by 11%. Table 4 results show that BC kriging is more robust in modelling Au in Wassa-Amenfi.

According to the coefficient of determination (R^2) in Table 4, the independent variable predicted 93 percent of the dependent variable in the BC Kriging model, indicating a perfect fit and a highly robust model. The results also show that BC kriging significantly improved log kriging Au concentration estimate by reducing the overall estimation error by 34% and increasing the coefficient of determination by 11%.

3.5 Gold Spatial Distribution

BC Kriging was used to forecast Au concentration at unsampled locations using a linear combination of observations from nearby sampled locations. Figure 4 shows the fitted gaussian semi-variogram model with a nugget effect of 0.1 and a nugget-to-sill variance of 0.52. The moderately high nugget-to-sill variance was caused by the banded nature of the mineralization, which is primarily due to the presence of impurities, specifically SiO_2 and Al_2O_3 , caused the moderately high nugget-to-sill variance.[27]

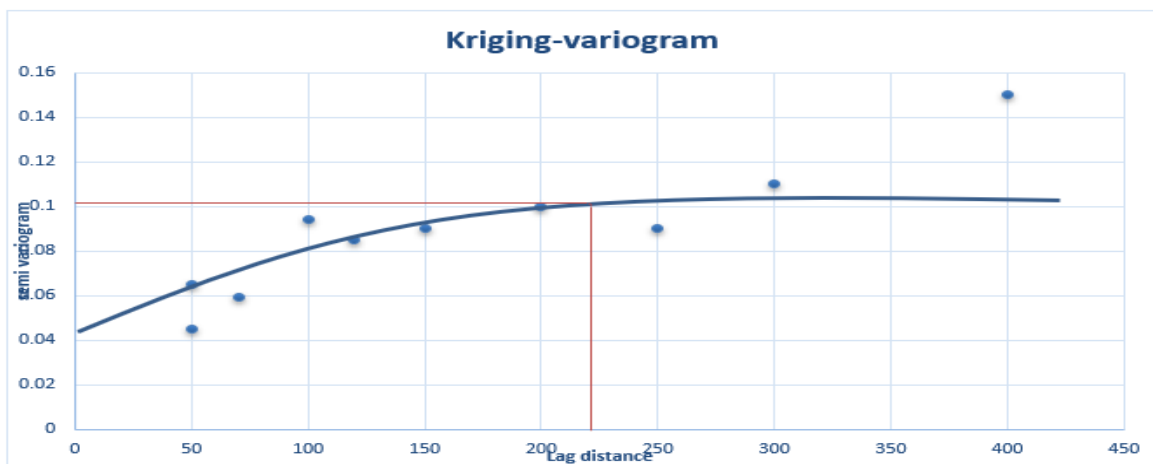


Figure 5: Semi-Variogram With Fitted Gaussian Model

Weights derived from the spatial covariance structure of the sampled points from the variogram were used to interpolate values for unsampled points across the spatial field, and the result is represented in contour a (Figure 6) and 3D surface (Figure 7) maps after determining the spatial covariance structure of the sampled points from the variogram.

The colour scale results in figures 6 and 7 were used to indicate where Au anomalies are located on the field. The red colour on the scales indicates areas with higher gold concentrations. According to [28], the Wasssa-Amenfi deposit is hosted in strongly sheared granitoid that are structurally controlled on the Asankrangwa belt, so the random distribution of Au anomalies was logical because this shear zone is not located in the study area's centre.

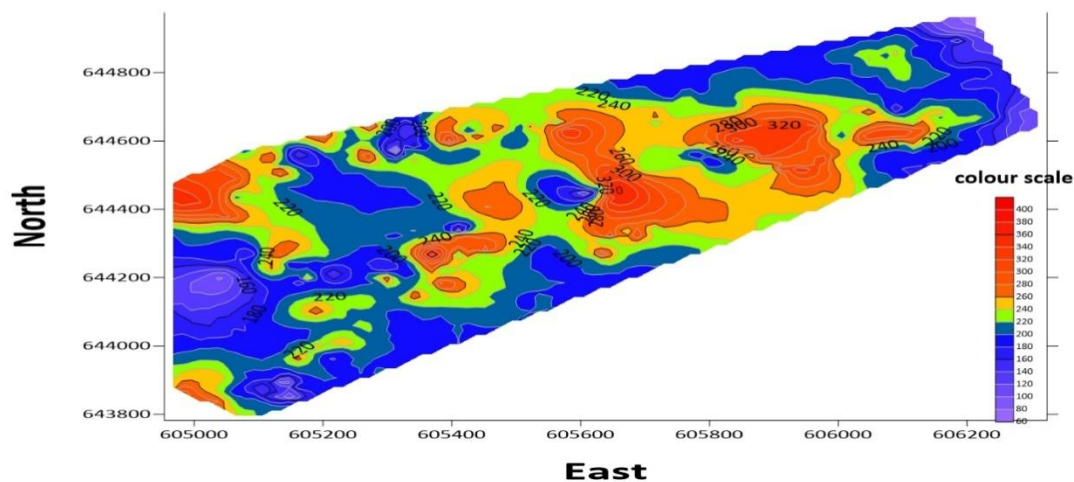


Figure 6: Delineation map for Au

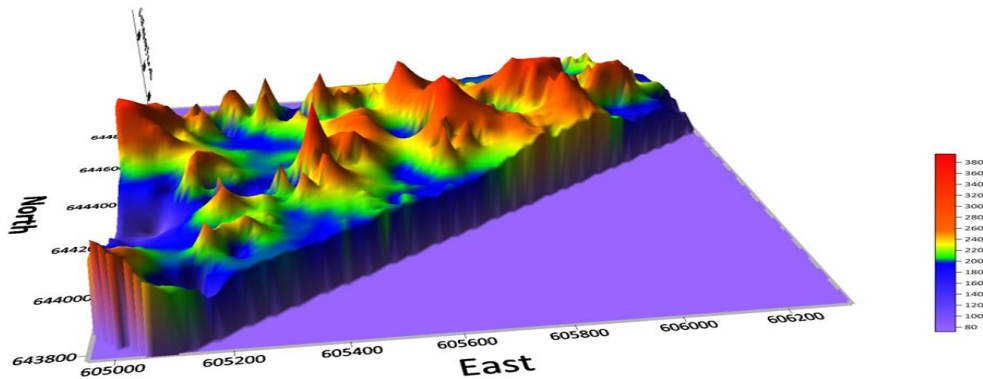


Figure 7:A surface map for Au.

4.0 CONCLUSION

Kriging and IDW methods were compared to determine the most robust spatial interpolation model. However, due to the strong spatial correlation structure of the dataset, the Kriging method outperformed the IDW method and was found to be the most effective in modelling the spatial distribution of gold within Wassa-Amenfi. Since gold grades were hosted within sheared zones of the granitoid. The much wider distribution of the Au anomalies zone, which was partly located in the study field's mid-portion, was logically possible as a result of a secondary dispersion mechanism that could have occurred regularly to change the vital constituent.

COMPETING INTERESTS DISCLAIMER:

Authors have declared that no competing interests exist. The products used for this research are commonly and predominantly used products in our area of research and country. There is no conflict of interest between the authors and producers of the products because we do not intend to use these products as an avenue for any litigation but the advancement of knowledge. Also, the research was not funded by the producing company rather it was funded by the personal efforts of the authors.

References

- [1]. Sinclair, A.J. and Blackwell, G.H., 2006. *Applied mineral inventory estimation*. Cambridge University Press.
- [2]. Wellmer, F.W., Dalheimer, M. and Wagner, M., 2007. *Economic evaluations in exploration*. Springer Science & Business Media.
- [3]. Ben-Daya, M., Duffuaa, S.O. and Raouf, A. eds., 2012. *Maintenance, modelling and optimization*. Springer Science & Business Media.
- [4]. Gol, M., Ghorbanian, D., Hassanzadeh, S., Javan, M., Mirnajafi-Zadeh, J. and Ghasemi-Kasman, M., 2017. Fingolimod enhances myelin repair of the hippocampus in the pentylenetetrazol-induced kindling model. *European Journal of Pharmaceutical Sciences*, 96, pp.72-83.
- [5]. Meyer, G., 2015. Commodity index investing debate reignites. *Financial Times*, <https://www.ft.com/content/9b307c8c-5d69-11e5-9846-de406ccb37f2>.
- [6]. Rossi, M.E. and Deutsch, C.V., 2013. *Mineral resource estimation*. Springer Science & Business Media.
- [7]. Lee, Y., Dominy, J.E., Choi, Y.J., Jurczak, M., Tolliday, N., Camporez, J.P., Chim, H., Lim, J.H., Ruan, H.B., Yang, X. and Vazquez, F., 2014. Cyclin D1–Cdk4 controls glucose metabolism independently of cell cycle progression. *Nature*, 510(7506), pp.547-551.
- [8]. The Role and Impact of Manazzamat Al-Dawa Al-Islamia Schools in Malawi from 2000-2006: A Case Study of Zomba and Mangochi Secondary School as-Salam Boys, as-Salam Girls, Al-Bakr Boys, and Aisha Girls Secondary School. *Kachere documents*.
- [9]. Harrison, S. and Sinclair, R., 2002. Telogen effluvium. *Clinical and Experimental Dermatology: Clinical dermatology*, 27(5), pp.389-395.
- [10]. Fotheringham, A.S. and O'Kelly, M.E., 1989. *Spatial interaction models: formulations and applications* (Vol. 1, p. 989). Dordrecht: Kluwer Academic Publishers.
- [11]. Burrough, P.A., 2001. GIS and geostatistics: Essential partners for spatial analysis. *Environmental and ecological statistics*, 8(4), pp.361-377.
- [12]. Lefaucheur, J.P., André-Obadia, N., Antal, A., Ayache, S.S., Baeken, C., Benninger, D.H., Cantello, R.M., Cincotta, M., de Carvalho, M., De Ridder, D. and Devanne, H., 2014. Evidence-based guidelines on the therapeutic use of repetitive transcranial magnetic stimulation (rTMS). *Clinical Neurophysiology*, 125(11), pp.2150-2206.
- [13] Amadu, C.C., Foli, G., Kissi-Abrokwa, B. and Akpah, S., 2021. Geostatistical Approach For The Estimation Of Shear-Hosted Gold Deposit: A Case Study Of The Obuasi Gold Deposit, Ghana. *Malaysian Journal of Geosciences (MJG)*, 5(2), pp.76-84.

- [14] Umar, U.S., Bello, A.M. and Munir, Z., Gold Geospatial Interpolations: Kriging versus Inverse Distance Weighting.
- [15].Goovaerts, P., 1997. *Geostatistics for natural resources evaluation*. Oxford University Press on Demand.
- [16] Xie, X., Wang, X., Zhang, Q., Zhou, G., Cheng, H., Liu, D., Cheng, Z. and Xu, S., 2008. Multi-scale geochemical mapping in China. *Geochemistry: Exploration, Environment, Analysis*, 8(3-4), pp.333-341.
- [17] Dzigbodi-Adjimah, K., 1993. Geology and geochemical patterns of the Birimian gold deposits, Ghana, West Africa. *Journal of geochemical exploration*, 47(1-3), pp.305-320.
- [18] Ren, Y., Yang, X., Hu, X., Wei, J. and Tang, C., 2022. Mineralogical and geochemical evidence for biogenic uranium mineralization in northern Songliao Basin, NE China. *Ore Geology Reviews*, 141, p.104556.
- [19] Wen, X.H., Capilla, J.E., Deutsch, C.V., Gómez-Hernández, J.J. and Cullick, A.S., 1999. A program to create permeability fields that honour single-phase flow rate and pressure data. *Computers & Geosciences*, 25(3), pp.217-230.
- [20] Cressie, N., 1988. Spatial prediction and ordinary kriging. *Mathematical Geology*, 20(4), pp.405-421.
- [21] Blenkinsop, T.G. and Kadzviti, S., 2006. Fluid flow in shear zones: insights from the geometry and evolution of ore bodies at Renco gold mine, Zimbabwe. *Geofluids*, 6(4), pp.334-345.
- [22] Bohling, G., 2005. Introduction to geostatistics and variogram analysis. *Kansas geological survey*, 1, pp.1-20.
- [23] Michel, F.C., 1982. Theory of pulsar magnetospheres. *Reviews of Modern Physics*, 54(1), p.1.
- [24] Zuo, R., 2011. Identifying geochemical anomalies associated with Cu and Pb–Zn skarn mineralization using principal component analysis and spectrum–area fractal modelling in the Gangdese Belt, Tibet (China). *Journal of Geochemical Exploration*, 111(1-2), pp.13-22.
- [25] Blanca, M.J., Arnau, J., López-Montiel, D., Bono, R. and Bendayan, R., 2013. Skewness and kurtosis in real data samples. *Methodology*.
- [26] Umar, U.S., Bello, A.M. and Munir, Z., Gold Geospatial Interpolations: Kriging versus Inverse Distance Weighting.
- [27] Schober, P., Boer, C. and Schwarte, L.A., 2018. Correlation coefficients: appropriate use and interpretation. *Anesthesia & Analgesia*, 126(5), pp.1763-1768
- [28] Chudasama, B., Porwal, A., Kreuzer, O.P. and Butera, K., 2016. Geology, geodynamics and orogenic goldprospectivity modelling of the Paleoproterozoic Kumasi Basin, Ghana, West Africa. *Ore Geology Reviews*, 78, pp.692-711.